A Trinuclear, Oxo-Centered Mixed-Valence Iron Complex with Unprecedented Carboxylate Coordination: $[Fe_3O(O_2CCH_3)_6(TACN)]\cdot 2CHCl_3$

Peter Poganiuch,[1a] Shuncheng Liu,[1a] Georgia C. Papaefthymiou,[1b] and Stephen J. Lippard*,[1a]

Contribution from the Department of Chemistry and the Francis Bitter National Magnet Laboratory, Massachusetts Institute of Technology, Cambridge, Massachusetts 02139.
Received December 7, 1990

Abstract: The trinuclear, oxo-centered mixed-valence complex $[Fe_3O(O_2CCH_3)_6(TACN)]\cdot 2CHCl_3$ (TACN = 1,4,7-triazacyclononane) was synthesized by air oxidation of ferrous acetate in the presence of TACN. The structure of the compound, determined by X-ray crystallography at 195 K, contains the well-known triangular $\{Fe_3O\}^{6+}$ core. Only one pair of adjacent Fe atoms is bridged by two bidentate acetate ligands, however, whereas the other two pairs are bridged by only one such ligand. The resulting isomer is unique among the extensive family of $[M^{III}_2M^{II}O(O_2CR)_6L_3]$ complexes. The terminal positions in the distorted octahedral coordination spheres of two of the three iron atoms are completed each by a rare bidentate acetate ligand, while the third iron atom is coordinated by a tridentate TACN ligand. Analysis of the iron–ligand bond lengths at each of the three metal atoms comprising the isosceles triiron(II,III,III) triangle reveals that $[Fe_3O(O_2CCH_3)_6(TACN)]\cdot 2CHCl_3$ is a localized mixed-valence compound at 195 K. The Fe–(μ-oxo) bond distances are 1.862 (4) and 1.867 (4) Å to the ferric ions and 1.998 (4) Å to the ferrous ion. Interestingly, the TACN ligand is coordinated to one of the trivalent iron centers, resulting in an asymmetric complex. The existence of this valence isomer is rationalized on the basis of intramolecular hydrogen bonding between the NH protons of the TACN ligand and the bidentate terminal acetate ligands, which seems to be optimized in the observed structure. The infrared spectrum shows resolved bands arising from the ν_{asym}(OCO) and ν_{sym}(OCO) vibrations of the bridging and terminal acetate ligands. Mössbauer spectroscopic studies of the compound reveal two resolved quadrupole doublets due to Fe(II) and Fe(III) at all temperatures in the range 4.2–295 K, confirming the valence-localized classification of the compound. Magnetic susceptibility measurements of $[Fe_3O(O_2CCH_3)_6(TACN)]\cdot 2CHCl_3$ from 2 to 300 K were well fit by a model having only two spin-exchange coupling constants $J_{13} = J_{23} = -16.5$ (4) cm^{-1} along the edges of the isosceles triangle joining the Fe(II)/Fe(III) pairs and $J_{12} = -41.8$ (10) cm^{-1} along the edge linking the two Fe(III) centers. The net antiferromagnetic coupling leads to an $S_T = 1$ ground state.

Trinuclear, oxo-centered carboxylate complexes have been known for over 80 years.[2] Of special interest are mixed valence species of general formula $[M^{II}M^{III}_2O(O_2CR)_6L_3]\cdot$sol, where M is a transition metal such as iron, chromium, or manganese, O_2CR is an aliphatic or halogen-substituted aliphatic carboxylate, L is a monodentate ligand such as water, pyridine, or substituted pyridine, and sol is a solvent molecule of crystallization. A comprehensive review of the chemical and physical properties of these triangular bridged complexes has recently appeared.[3]

The $Fe^{II}Fe^{III}_2$ complexes especially have been of considerable interest for examining the factors that influence the rates of electron transfer in mixed-valence compounds.[4] Examples of $[Fe^{II}Fe^{III}_2O(O_2CR)_6L_3]\cdot$sol compounds exist that are valence-localized[4,5] even above 300 K, whereas others undergo a transition from valence localization at low temperatures to valence delocalization at room temperature.[5]

The compounds known so far differ in the carboxylates, the monodentate ligand L, and the nature of the solvent of crystallization, but the structure of their $\{Fe_3O\}^{6+}$ cores has been invariant. The (μ-oxo)triiron(II,III,III) grouping is planar or approximately so, and the iron atoms are bridged pairwise by two bidentate carboxylate anions. The remaining position in the pseudooctahedral coordination sphere of each iron atom is occupied by a terminal monodentate ligand L.[3] For the case of a valence-delocalized compound, the core structure is that of an (nearly) equilateral triangle with all metal–ligand bonds equal (D_{3h} symmetry), whereas the valence-localized compounds have one iron atom structurally distinct from the other two (C_{2v} symmetry).[6]

In the course of our recent studies of the chemistry of ferrous carboxylates with nitrogen donor ligands and their reactions with dioxygen,[7] we discovered the unprecedented compound $[Fe_3O(O_2CCH_3)_6(TACN)]\cdot 2CHCl_3$ (**1**) (TACN = 1,4,7-triazacyclononane), the first example of a trinuclear, oxo-centered mixed-valence complex with a core different from that described above. The geometric relationship between this novel structural isomer (isomer B) and the previous class of compounds (isomer A), depicted below, arises from the use of the tridentate TACN ligand,

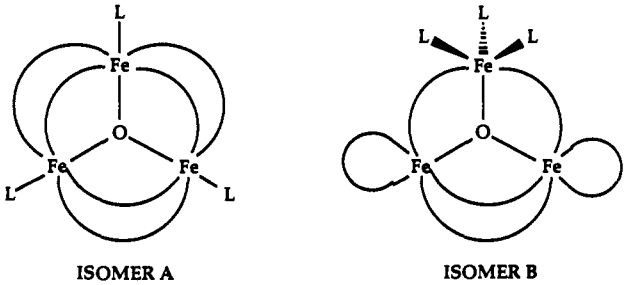

ISOMER A ISOMER B

which occupies a set of three facial coordination positions at one of the three vertices of the $\{Fe_3O\}^{6+}$ triangular core. Compound **1** is also of interest because of the presence of terminal chelating carboxylate ligands, a feature recently reported for the diiron(III)

(1) (a) Department of Chemistry. (b) Francis Bitter National Magnet Laboratory.

(2) (a) Weinland, R. F. *Chem.-Ztg.* **1908**, *32*, 812. (b) Werner, A. *Ber. Dtsch. Chem. Ges.* **1908**, *41*, 3447. (c) Cretien, A.; Lous, E. *Bull. Soc. Chim. Fr.* **1944**, *11*, 446.

(3) Cannon, R. D.; White, R. P. *Prog. Inorg. Chem.* **1988**, *36*, 195.

(4) See, for example, Jang, H. G.; Gelb, S. J.; Kaneko, Y.; Nakano, M.; Sorai, M.; Rheingold, A. L.; Montez, B.; Hendrickson, D. N. *J. Am. Chem. Soc.* **1989**, *111*, 173 and references cited therein.

(5) Oh, S. M.; Hendrickson, D. N.; Hassett, K. L.; Davis, R. E. *J. Am. Chem. Soc.*, **1985**, *107*, 8009.

(6) White, R. P.; Wilson, L. M.; Williamson, D. L.; Moore, G. R.; Jayasooriya, U. A.; Cannon, R. D. *Spectrochim. Acta* **1990**, *46A*, 917.

(7) (a) Tolman, W. B.; Bino, A.; Lippard, S. J. *J. Am. Chem. Soc.* **1989**, *111*, 4532. (b) Rardin, R. L.; Bino, A.; Poganiuch, P.; Tolman, W. B.; Liu, S.; Lippard, S. J. *Angew. Chem., Int. Ed. Engl.* **1990**, *29*, 812. (c) Tolman, W. B.; Liu, S.; Bentsen, J. G.; Lippard, S. J. *J. Am. Chem. Soc.* **1991**, *113*, 152.

0002-7863/91/1513-4645$02.50/0

oxo core in the B2 subunit of ribonucleotide reductase,[8] as well as the manner in which the electrons localize among the three iron centers. In the present paper, we describe the synthesis, X-ray crystal structure determination, and the results of magnetic susceptibility, infrared, and Mössbauer spectroscopic investigations of **1**.

Experimental Section

Materials and Methods. The ligand 1,4,7-triazacyclononane (TACN) was prepared according to a literature procedure.[9] All other reagents were obtained from commercial suppliers and used without further purification. All manipulations were carried out under argon or in a Vacuum Atmospheres glovebox. Electronic and Fourier transform infrared spectra were obtained on Varian Lambda 3 and Mattson Cygnus 400 instruments, respectively.

$[Fe_3O(O_2CCH_3)_6(TACN)]\cdot 2CHCl_3$ (1). A 0.3-g portion of TACN (2.3 mmol) and 1.253 g of $Fe(O_2CCH_3)_2$ (7.2 mmol) were suspended in 50 mL of methanol, whereupon the methanol solution turned slightly blue. The mixture was heated to 55 °C with stirring. The $Fe(O_2CCH_3)_2$ starting material dissolved completely within 15 min to give a clear pale green solution. After the solution was stirred for an additional 75 min at 55 °C, the methanol was removed in vacuo, leaving a colorless solid in the flask. A 120-mL portion of $CHCl_3$ was added to dissolve the solid, leaving only a small amount of insoluble material. Injection of 123 mL of air (~1.15 mmol of O_2) into the flask via syringe over a period of 1 h gave a brown solution, which was filtered. Slow diffusion of hexane vapor into the $CHCl_3$ filtrate yielded black-brown crystals of **1** within 2 days as well as a brown powder. The solids were separated from the solution by decanting. Hexane vapor was again allowed to diffuse into the solution, and after 2 days a second crop of crystals and brown powder were isolated. In the same manner, two more crops were obtained. Dark brown crystals of **1** were manually selected from the mixture of products with a dissecting needle, yielding 0.175 g (8.3%) of pure material and 0.280 g (13.5%) of almost pure crystals. An additional 0.27 g of brown crystals covered with the brown powder were also obtained. The compound was further purified by dissolving the crystals in $CHCl_3$ and again allowing hexane vapor to diffuse into the solution. IR (KBr, cm^{-1}): 3265, 3239, 3001 (w), 2976 (w), 2931 (w), 2876 (w), 1612 (s), 1592 (s), 1560 (s) (ν_{asym} CO_2), 1456 (sh), 1421 (s) (ν_{sym} CO_2), 1341, 1263 (s), 1237 (s), 1105, 1078, 1048, 1022, 964, 872 (w), 800 (w), 752, 677, 665, 657, 648, 616, 580 (w). UV/vis (CH_3CN solution (λ_{max}, nm (ϵ_M, M^{-1} cm^{-1}))): 220 (12 200), 310 (3650), 470 (sh), 723 (860). Anal. Calcd for $C_{20}H_{35}Cl_6Fe_3N_3O_{13}$: C, 26.52; H, 3.90; N, 4.64. Found: C, 26.82; H, 4.14; N, 4.44.

X-Ray Crystallography. A brown, block-shaped crystal of $[Fe_3O(O_2CCH_3)_6(TACN)]\cdot 2CHCl_3$ (dimensions 0.18 × 0.28 × 0.36 mm) was mounted on a glass fiber with epoxy resin. The crystal quality was found to be acceptable based on ω scans of several low-angle reflections ($\Delta\omega_{1/2}$ = 0.23°). Relevant crystallographic information is presented in Table I. Intensity data were collected on an Enraf-Nonius CAD4-F diffractometer by the general procedures previously described.[10] Corrections were applied for Lorentz and polarization effects, but it was unnecessary to correct for crystal decay and absorption. The structure was solved by using the direct methods (SHELXS) and standard difference Fourier routines in the TEXSAN package.[11] The positions of all non-hydrogen atoms were refined with anisotropic thermal parameters. The H atoms of the NH groups of TACN were located from difference Fourier maps. All other H atoms were placed at calculated positions for the final refinement cycles. Full-matrix least-squares refinement minimized the function $\sum w(|F_o| - |F_c|)^2$ and converged to the R factors reported in Table I. The largest peak in the final difference Fourier map had 0.62 e/Å^3 and was located near Cl3 of one of the solvent molecules. Selected bond distances and angles are provided in Table II. Full listings of bond distances and angles, positional parameters and B(eq) for all atoms, and anisotropic thermal parameters for all non-hydrogen atoms as well as observed and calculated structure factor amplitudes, are supplied as supplementary material (Tables S1–S5).

Magnetic Susceptibility Measurements. Solid-state magnetic susceptibilities of a powdered sample of **1** were measured between 2 and 300 K by using a Quantum Design SQUID magnetometer in the Department of Materials Science and Engineering at M.I.T. A plot of the magnetization of the sample vs field for data taken at 2.15 K was found to be linear only up to 4 kG. Data points between 4 and 10 K were therefore recorded at a field of 4 kG. Above 10 K, data could be taken at a field of 10 kG. A total of 46 data points was measured. The experimental moments were corrected for the magnetism of the sample holder, and a diamagnetic correction of -426×10^{-6} cm^3 mol^{-1}, calculated from Pascal's constants,[12] was applied. Table S6 reports observed molar suscep-

Table I. Crystallographic Information for $[Fe_3O(O_2CCH_3)_6(TACN)]\cdot 2CHCl_3$ (1)

formula	$C_{20}H_{35}Cl_6Fe_3N_3O_{13}$
formula weight, g mol^{-1}	905.77
crystal system	orthorhombic
space group	*Pbca*
a, Å	17.439 (4)
b, Å	18.290 (3)
c, Å	22.835 (3)
V, Å^3	7283 (4)
Z	8
T, K	195
ρ_{calc}, g cm^{-3}	1.652
ρ_{meas}, g cm^{-3} (295 K)[a]	1.65 (1)
radiation	Mo Kα (0.710 73 Å)
transmission factor range	0.927–1.00
data collected	$3° \le 2\theta \le 50°$, $+h$, $+k$, $+l$
total no. of data collected	7206
no. of unique data with $I > 3\sigma(I)$	3817
no. of variables	406
R[b]	0.048
R_w[c]	0.061

[a] Measured at room temperature in a mixture of CCl_4 and CH_2Br_2. [b] $R = \Sigma(|F_o| - |F_c|)/\Sigma|F_o|$. [c] $R_w = (\Sigma w(|F_o| - |F_c|)^2/\Sigma w|F_o|^2)^{1/2}$, where $w = 4F^2/\sigma^2(F^2)$ and $\sigma^2(F^2) = [(C + R^2B) + (pI)^2]/(Lp)^2$ with C = peak count, B = sum of left and right background counts, I = reflection intensity, Lp = Lorentz-polarization factor, and p = fudge factor, set equal to 0.05.

Table II. Selected Interatomic Distances (Å) and Angles (deg) for $[Fe_3O(O_2CCH_3)_6(TACN)]\cdot 2CHCl_3$ ($1\cdot 2CHCl_3$)[a]

Iron–Oxo Core			
Fe1–O	1.862 (4)	Fe1–O–Fe2	125.1 (2)
Fe2–O	1.867 (4)	Fe1–O–Fe3	122.2 (2)
Fe3–O	1.998 (4)	Fe2–O–Fe3	109.9 (2)
Fe1···Fe2	3.310 (1)	Fe1–Fe2–Fe3	62.88 (3)
Fe2···Fe3	3.166 (1)	Fe1–Fe3–Fe2	60.65 (3)
Fe1···Fe3	3.380 (1)	Fe2–Fe1–Fe3	56.47 (3)

TACN Ligand

			min	max
Fe1–N1	2.180 (5)	N–C	1.463	1.496
Fe1–N2	2.172 (5)	C–C	1.51	1.52
Fe1–N3	2.210 (5)	N–C–N	112.7	114.0

Bridging Acetate Ligands

Fe1–O1	2.009 (4)	Fe2–O2	2.065 (5)	Fe3–O9	2.128 (5)
Fe1–O10	1.981 (4)	Fe2–O5	1.966 (5)	Fe3–O6	2.113 (5)
		Fe2–O7	2.032 (5)	Fe3–O8	2.061 (5)
average	1.99	average	2.02	average	2.10
O1–C1–O2	126.1 (6)	O7–C7–O8	126.0 (6)		
O5–C5–O6	125.5 (6)	O9–C9–O10	124.8 (6)		

Terminal Acetate Ligands

Fe2–O3	2.124 (5)	Fe3–O12	2.282 (5)
Fe2–O4	2.205 (5)	Fe3–O11	2.136 (4)
average	2.165	average	2.209
O3–Fe2–O4	60.4 (2)	O11–Fe3–O12	59.7 (2)
O3–C3–O4	119.7 (6)	O11–C11–O12	120.6 (6)

Hydrogen Bonds

N1···O3	2.844 (7)	N2···O12	2.895 (7)
N1–H1	1.073	N2–H2	1.111
H1–O3	1.809	H2–O12	1.824
N1–H1–O3	155.2	N2–H2–O12	160.6

[a] See Figure 1 for atom-labeling scheme. Numbers in parentheses are estimated standard deviations in the last digit(s).

(8) Nordlund, P.; Sjöberg, B.-M.; Eklund, H. *Nature* **1990**, *395*, 593.
(9) Wieghardt, K.; Schmidt, W.; Nuber, B.; Weiss, J. *Chem. Ber.* **1979**, *112*, 2220.
(10) Silverman, L. D.; Dewan, J. C.; Giandomenico, C. M.; Lippard, S. J. *Inorg. Chem.* **1980**, *19*, 3379.
(11) *TEXRAY Structure Analysis Package*; Molecular Structure Corporation: College Station, TX, 1985.
(12) R. R. Gupta *Landolt-Börnstein, New Series II/16*; Springer-Verlag: Berlin 1986, p 1 ff.

Table III. Comparison of Distances (Å) and Angles (deg) of the Terminal Bidentate Acetate Ligands in **1**, $[Fe(O_2CCH_3)Cl(BIPhMe)]$ (**2**),[17] and $[Fe(O_2CCH_3)_2(2,9\text{-}(CH_3)_2\text{-}o\text{-phen})]\cdot 0.5THF$ (**3**)[17]

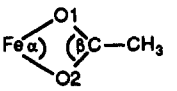

compd	n^a	Fe–O1	Fe–O2	ave Fe–O[b]	O1–C	O2–C	C–CH_3	α	β
1, Fe(III) site	6	2.124 (5)	2.205 (5)	2.165	1.275 (9)	1.245 (9)	1.49 (1)	60.4 (2)	119.7 (6)
1, Fe(II) site	6	2.282 (5)	2.136 (4)	2.21	1.258 (8)	1.276 (8)	1.49 (1)	59.7 (2)	120.6 (6)
2	5	2.103 (3)	2.196 (3)	2.15	1.206 (6)	1.234 (5)	1.53 (1)	59.7 (1)	122.7 (4)
3, ligand 1	6	2.065 (3)	2.347 (4)	2.21	1.261 (6)	1.241 (6)	1.51 (1)	58.5 (1)	118.8 (4)
3, ligand 2	6	2.110 (3)	2.258 (4)	2.18	1.251 (6)	1.246 (5)	1.50 (1)	59.4 (1)	120.6 (4)

[a] Coordination number. [b] Average Fe–O distance.

tibilities and their estimated errors.

Results and Discussion

Synthesis. The mixed-valence compound $[Fe_3O(O_2CCH_3)_6(TACN)]\cdot 2CHCl_3$ forms by air oxidation of an intermediate ferrous complex. When methanol is added to a 3:1 mixture of $Fe(O_2CCH_3)_2$ and TACN under argon, the latter dissolves almost immediately, whereas the former remains mostly undissolved. The color of the solution turns slightly blue, probably because of the formation of $[Fe(TACN)_2]^{2+}$, which is reported to be blue.[13] When the slurry is heated to 55 °C, $Fe(O_2CCH_3)_2$ dissolves over time and the color of the solution changes to pale green. One or more thus far unidentified ferrous products form. Several attempts to crystallize these species were unsuccessful.

The $CHCl_3$ solution was oxidized with the stoichiometric amount of air required to convert $^2/_3$ of the Fe(II) present to Fe(III). In the course of the oxidation, **1** forms together with other Fe(III) products in low yield (<30%). The oxidative self-assembly reaction yielding **1** is analogous to the formation of the mixed-valence compound $[Fe_3O(O_2CCH_3)_6(H_2O)_3]$, which is similarly obtained by air oxidation of $FeCl_2\cdot 4H_2O$ in NaO_2CCH_3/CH_3COOH solution[5,14] in 53% yield or in $Ca(O_2CCH_3)_2$ solution in 69% yield.[2,15]

Because of the low yield, we tried to develop alternative synthetic routes to **1** via substitution reactions. Addition of TACN to $[Fe_3O(O_2CCH_3)_6(H_2O)_3]$ (1:1 ratio) in $CHCl_3$ under Ar did afford **1**, but in a yield of only 1%. The major product of this reaction appears to be an ionic adduct of TACN with $[Fe_3O(O_2CCH_3)_6(H_2O)_3]$, judging from its solubility properties. IR spectroscopy revealed that the product(s) still contains water. The reaction of $[Fe_3O(O_2CCH_3)_6(py)_3]$[14] with TACN in $CHCl_3$ also gave only oils. Thus, the route reported above appears to be the best, if not the only, way to obtain reasonable quantities of pure, crystalline **1**.

Description of the Structure. An ORTEP representation of the structure of $[Fe_3O(O_2CCH_3)_6(TACN)]$ is presented in Figure 1, and selected interatomic distances and angles are listed in Table II. The central Fe_3O unit of the complex is nearly planar, with the bridging μ_3-oxo atom displaced by only 0.18 Å from the plane defined by the three iron atoms. The triangle of iron atoms is isosceles rather than equilateral, with the shortest Fe···Fe distance (3.166 (1) Å) occurring between Fe2 and Fe3 and the Fe1···Fe2 (3.310 (1) Å) and Fe1···Fe3 (3.380 (1) Å) distances being significantly longer.

The most striking difference between the previously known triangular mixed-valence iron cmpounds and the present compound is the coordination mode of the acetate ligands. In **1**, only Fe2 and Fe3 are linked by two bidentate (syn–syn) acetate groups, whereas the Fe1–Fe2 and Fe1–Fe3 pairs are bridged by only one such ligand. The remaining positions in the coordination spheres of both Fe2 and Fe3 are occupied by bidentate terminal acetate ligands. Carboxylate ligands coordinated in a bidentate fashion

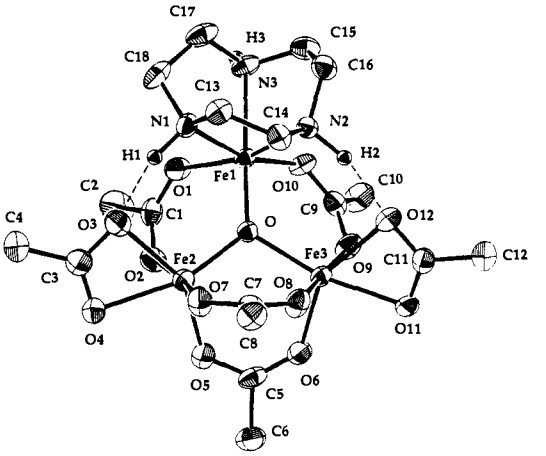

Figure 1. Structure of **1** showing the 50% probability thermal ellipsoids and the atom-labeling scheme. All but the three TACN hydrogen atoms were omitted for clarity.

to one metal center are rare compared to bridging carboxylates. Only a few examples have thus far been cited in the literature and none for iron.[16] Thus, **1** affords the first opportunity to examine bond lengths and angles for this unit, which as previously stated has recently been found at the dinuclear iron oxo core in the B2 subunit of ribonucleotide reductase.[8] In addition to **1**, chelating terminal acetate ligands have been structurally characterized in both $[Fe(O_2CCH_3)Cl(BIPhMe)]$ (**2**), where BIPhMe = 2,2′-bis(1-methylimidazolyl)phenylmethoxymethane), and $[Fe(O_2CCH_3)_2(2,9\text{-dimethyl-}o\text{-phen})]$ (**3**).[17] Results for these Fe(II) and Fe(III) complexes are included for comparison purposes in Table III.

The coordination sphere of Fe1 is completed by the tridentate, facially coordinating ligand TACN. The occurrence of the novel isomer B in the present compound, compared with isomer A found in all previously characterized $[M^{II}M^{III}_2O(O_2CR)_6L_3]\cdot sol$ compounds, is the direct result of the use of a tridentate chelating TACN molecule as the "L_3" unit. As reported earlier for dinuclear (μ-oxo)bis(μ-carboxylato)diiron(III) complexes of TACN[18] and other tridentate facially coordinating ligands,[19] the Fe1–N3 bond trans to the Fe1–O bond in **1** is significantly longer than the cis Fe1–N1 and Fe1–N2 bonds, 2.210 (5) Å as compared to the values of 2.180 (5) and 2.172 (5) Å, respectively.

(13) Wieghardt, K.; Schmidt, W.; Herrmann, W.; Küppers, H. J. *Inorg. Chem.* **1983**, *22*, 2953.
(14) Meesuk, L.; Jayasooriya, U. A.; Cannon, R. D. *J. Am. Chem. Soc.* **1987**, *109*, 2009.
(15) Dziobkowski, C. T.; Wrobleski, J. T.; Brown, D. B. *Inorg. Chem.* **1981**, *20*, 679.
(16) (a) van Niekerk, J. N.; Schoening, F. R. L.; Talbot, J. H. *Acta Cryst.* **1953**, *6*, 720. (b) Zachariasen, W. H.; Plettinger, H. A. *Acta Crystallogr.* **1959**, *12*, 526. (c) Dean, W. K.; Simon, G. L.; Treichel, P. M.; Dahl, L. F. *J. Organomet. Chem.* **1973**, *50*, 193. (d) Drew, M. G. B.; Othman, A. H.; Edwards, D. A.; Richards, R. *Acta Crystallogr.* **1975**, *B31*, 2695. (e) Alcock, N. W.; Tracy, V. M. *J. Chem. Soc., Dalton Trans.* **1976**, 2246. (f) La Monica, G.; Cenini, S.; Formi, E.; Manassaro, M.; Albano, V. G. *J. Organomet. Chem.* **1976**, *112*, 297.
(17) Poganiuch, P.; Liu, S.; Lippard, S. J. To be submitted for publication.
(18) (a) Wieghardt, K.; Pohl, K.; Gebert, W. *Angew. Chem.* **1983**, *95*, 739. (b) Spool, A.; Williams, I. D.; Lippard, S. J. *Inorg. Chem.* **1985**, *24*, 2156.
(19) (a) Armstrong, W. H.; Spool, A.; Papaefthymiou, G. C.; Frankel, R. B.; Lippard, S. J. *J. Am. Chem. Soc.* **1984**, *106*, 3653. (b) Gomez-Romero, P.; Casan-Pastor, N.; Ben-Hussein, A.; Jameson, G. B. *J. Am. Chem. Soc.* **1988**, *110*, 1988.

The metrical parameters (Table II) of **1** at 195 K are consistent only with a localized mixed-valence compound, because the Fe(II) center can be unambiguously distinguished from the two Fe(III) atoms by the bond lengths within its coordination sphere. Interestingly, the Fe(II) atom, namely, Fe3, is not the one coordinated to the TACN nitrogen donor ligand, which instead is bonded to Fe1. Comparison of the three Fe-(μ-oxo) distances clearly reveals the Fe3–O bond (1.998 (4) Å) to be 0.14 Å longer than the Fe1–O (1.862 (4) Å) and the Fe2–O (1.867 (4) Å) bonds. The values agree well with those found in the localized mixed-valence compound $[Fe_3O(O_2CCH_3)_6(4\text{-Et-py})_3]\cdot 4\text{-Et-py}$,[5] for which an Fe(II)–O distance of 2.010 (4) Å and two Fe(III)–O distances of 1.856 (7) Å were reported. Furthermore, the average Fe–O bond length between iron and the oxygen atoms of the bridging carboxylate ligands is larger for Fe3 than for Fe1 and Fe2 (see Table II) as is the average Fe–O distance between Fe and the terminal acetate ligands. The occurrence of longer iron–ligand bond distances in the coordination sphere of Fe3 leaves little doubt that Fe3 is the ferrous and that Fe1 and Fe2 are the ferric iron atoms. Finally, the Fe1–N distances of 2.17–2.21 Å are in good accord with the values of 2.16–2.21 Å found earlier for these bonds in the dinuclear ferric complex $[Fe_2O(O_2CCH_3)_2(TACN)_2]^{2+}$.[18]

Another structural parameter of interest is the Fe–O–Fe bond angle involving the bridging oxo ligand, of which there are two classes (Figure 1, Table II). The smallest of the three values occurs for Fe2–O–Fe3, along the short edge of the isosceles triangle. This result is ascribed to the presence of three bridging ligands, two carboxylates, and the μ-oxo group linking Fe2 and Fe3, whereas the other two pairs of iron atoms are bridged only by a μ-oxo and a single carboxylate group. A similar trend in Fe–O–Fe angles occurs for oxo-bridged diiron(III) complexes.[20]

The structure of **1** is stabilized by internal hydrogen bonds (Figure 1). The N1···O3 and N2···O12 distnaces between the TACN nitrogen atoms on Fe1 and the terminal acetate ligands coordinated at Fe2 and Fe3, respectively, are less than 2.90 Å (Table II). Such values are indicative of hydrogen-bonding interactions.[21] Independent evidence for the existence of these hydrogen bonds is provided by the infrared spectrum of **1** (Figure 2). Two bands occur at 3265 and 3239 cm^{-1}, which arise from the N–H stretching vibrations of the TACN ligand,[22] indicating the presence of two different types of secondary amine N–H bonds. It is well-known that hydrogen bonding diminishes the X–H (X = O, N) stretching frequencies in the IR spectrum.[23] We therefore assign the less intense, higher energy band at 3265 cm^{-1} to the N3–H3 stretching vibration. Examination of the crystal structure reveals H3 not to be involved in hydrogen bonding. The more intense band at 3239 cm^{-1}, which is shifted by 24 cm^{-1} to lower frequency, is due to the N1–H1 and N2–H2 vibrations, for which the crystal structure indicates hydrogen bonding (Figure 1).

The hydrogen bonding between NH protons of TACN and the terminal chelating carboxylate groups affords a rationale for understanding why one of the two Fe(III) ions in **1** prefers to occupy the position where the tridentate nitrogen ligand is coordinated. In this valence isomer, the Fe–(μ-oxo) bond length is significantly shorter (0.134 Å) than if a divalent iron were to occupy that position. This difference results in ~0.05 Å shorter contacts between the amine nitrogen donor and acetate acceptor partners participating in the internal hydrogen bonds, as revealed by molecular graphics calculations with the CAChe system of programs.[24] Although the energetics involved are small, they are probably sufficient to localize the structure to the asymmetric isomer B found for **1**, since previous work has shown that even such subtle factors as crystal packing forces and temperature-dependent solvent reorientations can affect the internal electron-transfer reactions of compounds in this class having isomer A.[3-5]

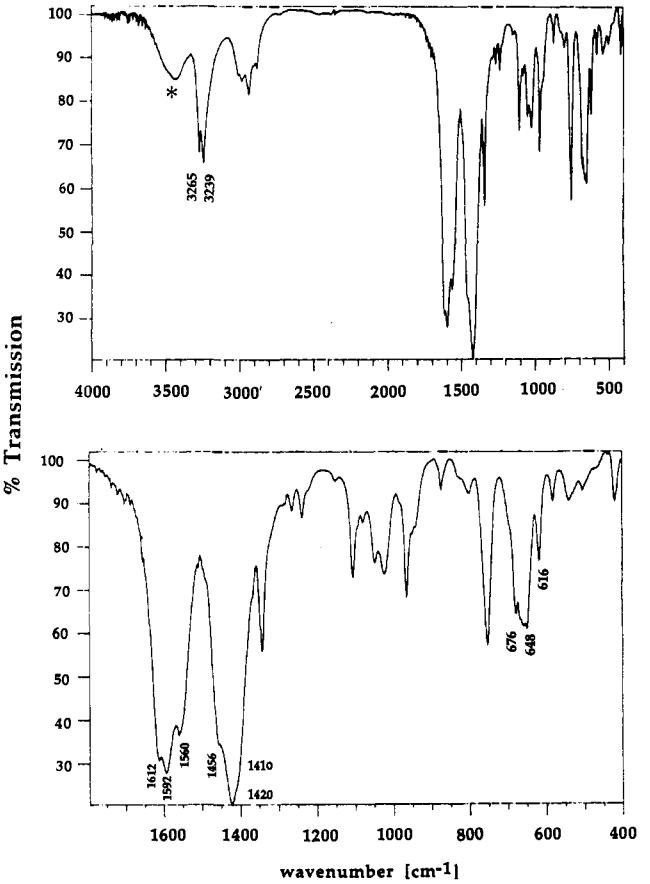

Figure 2. FT-IR spectrum of **1** at 295 K between 4000 and 400 cm^{-1} (top) and between 1800 and 400 cm^{-1} (bottom). The broad peak at ~3450 cm^{-1} marked with an asterisk is due to water present in the KBr and did not appear in other samples.

An additional point of interest that emerged during the analysis of the hydrogen-bonding interactions is the prediction that the 1,4,7-trimethyl-1,4,7-triazacyclononane (Me_3TACN) analogue of **1** would be unstable. As can be seen from Figure 1, replacement of the hydrogen atoms on N1 and N2 with methyl groups would lead to pronounced steric clashes with the acetate oxygen atoms O3 and O12. Replacement of hydrogen by methyl groups in these positions (N–C 1.42 Å) in the CAChe molecular modeling program resulted in $CH_3\cdots O$ distances of 1.5 Å, far less than the sum of the van der Waals radii (3.4 Å).

Infrared Spectroscopy. The IR spectra of carboxylate complexes are usually dominated by two strong bands between 1350 and 1650 cm^{-1} arising from the carbon–oxygen stretching vibrations. The frequency difference ($\Delta\nu$) between the symmetric ($\nu_{sym}(CO_2)$, typically between 1400 and 1450 cm^{-1}) and asymmetric ($\nu_{asym}(CO_2)$, typically between 1550 and 1650 cm^{-1}) C–O vibrations is correlated with the coordination mode of a carboxylate ligand.[25]

In the IR spectrum of **1** (Figure 2), bands due to acetate in different coordination modes are well resolved. Three $\nu_{asym}(CO_2)$ bands are found at 1612, 1592, and 1560 cm^{-1}, and at least two $\nu_{sym}(CO_2)$ bands are resolved at 1456 and 1420 cm^{-1}. In addition, a shoulder appears around 1410 cm^{-1}. There are six ways to calculate $\Delta\nu$ pairwise from these values, and in the absence of

(20) Kurtz, D. M., Jr. *Chem. Rev.* **1990**, *90*, 585.
(21) Olovsson, I.; Jönsson, P. G. In *The Hydrogen Bond*; Schuster, P., Zundel, G., Sandorfy, C., Eds.; North Holland: Amsterdam, 1976; Vol. II, p 395 ff.
(22) Socrates, G. *Infrared Characteristic Frequencies*; Wiley: New York, 1980.
(23) Hadzi, D.; Bratos, S. In *The Hydrogen Bond*; Schuster, P., Zundel, G., Sandorfy, C., Eds.; North Holland: Amsterdam, 1976; Vol. II, pp 567 ff.
(24) These calculations were performed with the CAChe stereo molecular modeling system, Version 2.2, Tektronix, Inc., Beaverton, OR.
(25) For details, see the following review articles: (a) Mehrotra, R. C.; Bohra, R. *Metal Carboxylates*; Academic Press: London, 1983; p 48 ff. (b) Deacon, G. B.; Philips, R. J. *Coord. Chem. Rev.* **1980**, *33*, 227.

Table IV. Mössbauer Parameters for $[Fe_3O(O_2CCH_3)_6(TACN)]\cdot 2CHCl_3$ ($1\cdot 2CHCl_3$)[a]

	δ (mm/s)		ΔE_Q (mm/s)		Γ (mm/s)	
T (K)	Fe^{II}	Fe^{III}	Fe^{II}	Fe^{III}	Fe^{II}	Fe^{III}
4.2	1.35 (1)	0.56 (1)	2.93 (1)	0.89 (1)	0.32 (3)	0.30 (3)
80	1.23 (1)	0.54 (1)	2.66 (1)	0.89 (1)	0.30 (3)	0.30 (3)
200	1.00 (1)	0.53 (1)	2.30 (1)	0.79 (1)	0.33 (3)	0.33 (3)
250	0.84 (1)	0.53 (1)	2.00 (1)	0.715 (1)	0.32 (3)	0.34 (3)
295	0.80 (1)	0.54 (1)	1.99 (1)	0.64 (1)	0.31 (3)	0.33 (3)

[a] The isomer shift (δ) is reported relative to iron metal at room temperature.

further information a unique assignment is not possible. According to the literature,[25] values of $\Delta\nu$ significantly lower than 160 cm^{-1} are indicative of chelate formation. A reasonable possibility is that the two bands at 1456 and 1560 cm^{-1}, with $\Delta\nu$ of only 104 cm^{-1}, are the $\nu_{asym}(CO_2)$ and the $\nu_{sym}(CO_2)$ vibrations of the chelating acetate ligands at Fe2 and Fe3. The two remaining $\Delta\nu$ values are within the range reported for bridging carboxylates, but again an unambiguous assignment cannot be made. An attempt to analyze the bond lengths and angles from the crystal structure in detail did not permit a distinct correlation to be drawn.

Different carboxylate coordination modes are also manifest in the spectral region between 600 and 700 cm^{-1}, in which the IR spectrum of **1** reveals one band at 616 cm^{-1} and several others between 648 and 676 cm^{-1}. Vibrational spectra of a large number of triangular complexes, such as mixed-valence $[Fe_3O(O_2CCH_3)_6L_3]$,[14,26] triiron(III) $[Fe_3O(O_2CCH_3)_6L_3]^+$,[14,27] and mixed-metal $[Fe^{III}_2M^{II}O(O_2CCH_3)_6L_3]$[14] species, have been analyzed in the past. All complexes exhibit the symmetric O–C–O deformation mode (δ(OCO)) between 650 and 690 cm^{-1}. We therefore assign the bands between 648 and 676 cm^{-1} in **1** to the δ(OCO) vibrations of at least the bridging acetate ligands. To our knowledge, no detailed vibrational analysis for a complex containing terminal acetate ligands has thus far been carried out. Two complexes having terminal acetate ligands ($[Fe(O_2CCH_3)Cl(BIPhMe)]$ and $[Fe(O_2CCH_3)_2(2,9\text{-}(CH_3)_2\text{-}o\text{-}phen)]$[17] recently prepared in our laboratory, however, exhibit infrared spectral bands at 646 and 650 cm^{-1}, respectively. We therefore conclude that the δ(OCO) vibrations for terminal acetate ligands also contribute to the bands between 648 and 676 cm^{-1}. According to the literature,[13,26,27] the band at 616 cm^{-1} can be assigned to the O–C–O out-of-plane deformation mode (π(COO)). It is not surprising that, unlike the δ(OCO) deformations, this band is not split because the vibrational analysis mentioned above revealed the π(COO) vibration to be minimally influenced by coordination to different metals or to the same metal in different oxidation states. In all compounds investigated, it appeared between 614 and 619 cm^{-1}.

Mössbauer Spectroscopy. Mössbauer spectra of **1** in the 4.2–295-K temperature range reveal localized Fe(III) and Fe(II) sites with an intensity ratio of ~2:1 (Figure 3). The Mössbauer parameters obtained from least-squares fits of the experimental data to Lorentzian lines are collected in Table IV. The values at 80 K are typical for high-spin ferric ($S = {}^5/_2$) and high-spin ferrous ($S = 2$) ions.[28] The crystal structure of **1** unambiguously reveals two different Fe(III) sites, one having six O-donor ligands and the other three O- and three N-donor atoms. The Mössbauer parameters of these two ferric sites are so similar, however, that separate quadrupole doublets could not be resolved. One might have expected different electric field gradients (EFG's) at Fe1 and Fe2 arising from their different coordination geometries and ligand identities. For example, in the asymmetric oxo-bridged trinuclear ferric complex $[Fe_3O(TIEO)_2(O_2CPh)_2Cl_3]$, which has two distinct ferric sites, two quadrupole doublets could be resolved.[29] On the other hand, the isomer shifts and quadrupole

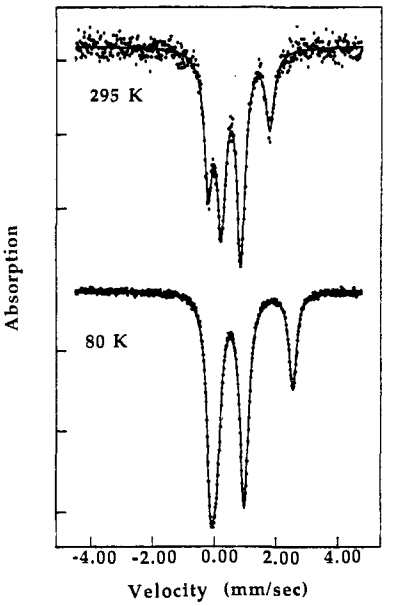

Figure 3. Mössbauer spectra of **1** at 80 and 295 K. The solid line is the theoretical simulation from use of the parameters in Table IV.

splitting parameters in $[Fe_2O(O_2CCH_3)_2(HB(pz)_3)_2]$[30] and $[Fe_2O(O_2CCH_3)_2\{OP(OEt)_2\}_3Co(C_5H_5)\}_2]$,[31] which have FeN_3O_3 and FeO_6 coordination spheres, respectively, are quite similar to one another. Thus, the inability to resolve separate Mössbauer parameters for Fe1 and Fe2 in **1** is perhaps not unexpected.

The quadrupole splitting of the high-spin ferric component of the spectrum shows a pronounced and unusual temperature dependence, while the temperature-dependent quadrupole splitting exhibited by the ferrous subsite is consistent with that expected for high-spin Fe(II).[28] On the other hand, the variation of the isomer shift of the ferrous site is much greater than anticipated from the second-order Doppler shift, which arises from thermal excitations of vibronic states of an otherwise unmodified crystal lattice.[30] By contrast, the isomer shift of the ferric sites is independent of temperature. Significantly, no line broadening beyond that due to instrumental factors[31] is evident throughout the temperature region studied.

The pronounced diminution in the isomer shift of the Fe(II) center in **1** with increasing temperature and the insensitivity of the isomer shifts of the Fe(III) sites to temperature are consistent with a shift in electron density from Fe(II) to Fe(III). Such an electronic redistribution, which probably occurs via the Fe–(μ-oxo) bonds, can also explain the observed temperature dependence of the quadrupole splitting parameter for the ferric sites. The ΔE_Q values in (μ-oxo)bis(μ-carboxylato)diiron(III) complexes are very sensitive to the Fe–O bridge bond length, reflecting the degree of orbital overlap between the bridging oxygen ligand and the iron atoms.[32] A very similar temperature-dependent isomer shift of the ferrous site has also been observed for the mixed-valence compound $[Fe_3O(O_2CCH_3)_6(4\text{-Etpy})_3]\cdot 4\text{-Et-py}$,[5] which is localized on the Mössbauer time scale and also exhibits sharp resonance lines. In this case, a disordered 4-Et-py ligand, associated with cooperative intermolecular effects in the solid state, was presumed to bring about the unusual temperature dependence of the Mössbauer parameters. The crystal structure of **1** shows no sign of disordered ligands or solvent molecules, however. Thus, a similar mechanism cannot be invoked in the present case. In

(26) Montri, L.; Cannon, R. D. *Spectrochim. Acta* **1985**, *41A*, 643.
(27) Johnson, M. K.; Powell, D. B.; Cannon, R. D. *Spectrochim. Acta* **1981**, *37A*, 995.
(28) Greenwood, N. N.; Gibb, T. C. *Mössbauer Spectroscopy*; Chapman & Hall: London, 1971.
(29) Gorun, S. M.; Papaefthymiou, G. C.; Frankel, R. B.; Lippard, S. J. *J. Am. Chem. Soc.* **1987**, *109*, 4244.
(30) Vertes, A.; Korecz, I.; Burger, K. *Studies in Physical and Theoretical Chemistry, Mössbauer Spectroscopy*; Elsevier: Amsterdam, 1979; Vol. 5, p 36 ff.
(31) The minimum line width that can be obtained with our instrumentation is ~0.30 mm/s, as found by calibration measurements with α-iron foil.
(32) (a) Armstrong, W. H.; Lippard, S. J. *J. Am. Chem. Soc.* **1984**, *106*, 4632. (b) Wu, F. J.; Kurtz, D. M., Jr.; Hagen, K.; Nyman, P.; Debrunner, P. G.; Vankai, V. *Inorg. Chem.* **1990**, *29*, 5174.

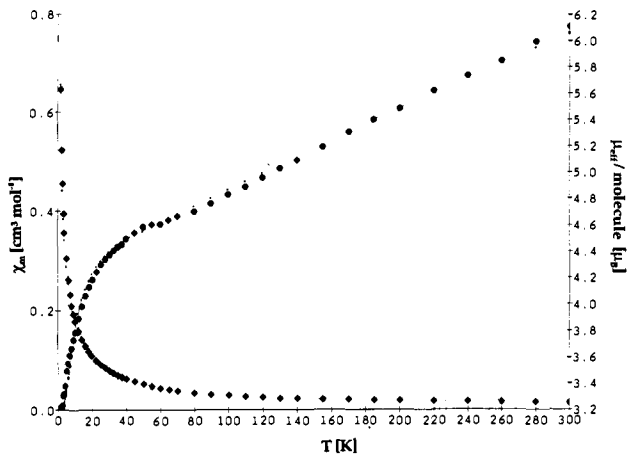

Figure 4. Plot of the molar suceptibility (χ_M) and the effective moment (μ_{eff}) per molecule for solid **1**. Dashed lines represent the results of least-square fits (see text).

general, investigations of mixed-valence compounds of the type $[Fe_3O(O_2CCH_3)_6L_3]$·sol have revealed complicated physical behavior where even small changes in the lattice result in dramatic changes in a measured parameter.[4,5,33]

The observation of resolved quadrupole doublets for the ferric and the ferrous sites confirms the results of the X-ray structure analysis. Compound **1** is clearly a localized mixed-valence species, belonging to class I of the Robin and Day scheme.[34]

Magnetic Behavior. Figure 4 shows plots of the molar susceptibility (χ_M) and effective moment (μ_{eff}) per molecule, calculated[35] from χ_M by the expression $\mu_{eff} = 2.828(\chi_M T)^{1/2}$, of **1** as a function of temperature. The theoretical spin-only moment in the absence of any coupling is 9.70 μ_B/molecule. At 300 K, the measured effective moment is only 6.11 μ_B/molecule, indicating net antiferromagnetic exchange coupling. This value is slightly larger than those previously reported for $[Fe^{II}Fe^{III}_2O(O_2CR)_6L_3]$ mixed-valence compounds (5.27–5.89 μ_B/molecule).[3,36] Upon cooling of **1**, the moment reduces to 3.21 μ_B/molecule at 2 K, consistent with an $S = 1$ ground state, the theoretical value for which is 2.83 μ_B/molecule. The assignment of this ground state was confirmed by successfully fitting the detailed temperature dependence of the magnetic susceptibility data.

In principle, the ground state of a molecule with two high-spin Fe(III) ($S = {}^5/_2$) and one high-spin Fe(II) ($S = 2$) centers can have total spin (S_T) values ranging from 0 to 7. The interaction of three magnetic ions in a cluster with one another and the magnetic field, assuming isotropic exchange coupling, is governed by the Hamiltonian given in eq 1.[37] A rigorous theoretical

$$\mathcal{H} = -2(J_{12}\mathbf{S}_1\cdot\mathbf{S}_2 + J_{13}\mathbf{S}_1\cdot\mathbf{S}_3 + J_{23}\mathbf{S}_2\cdot\mathbf{S}_3) + \mu_B(g_1\mathbf{S}_1 + g_2\mathbf{S}_2 + g_3\mathbf{S}_3)\cdot\mathbf{H} \quad (1)$$

treatment of the susceptibility of **1** should in principle employ the full Hamiltonian because all iron atoms in **1** are inequivalent. Unfortunately, without simplifying assumptions, the solution is complicated and has only been accomplished previously for trimetallic centers by assuming equal g factors.[38] In the present case, however, it cannot be presumed that the g values for the Fe(II) and Fe(III) atoms are equivalent.

The problem can be simplified, however, by using the results of Blake et al., who showed that the μ_3-oxo atom provides the main superexchange pathway in trinuclear carboxylate complexes, whereas exchange via the bridging carboxylates can be largely neglected.[39] The value of J is mainly determined by the Fe–O bond length, which modulates the degree of orbital overlap between the bridging oxo ligand and the iron centers.[40] The exchange parameter J is also influenced by the Fe–O–Fe angle, but only to a minor extent.[41] A similar correlation has been independently discovered empirically for a variety of polyiron oxo complexes.[42] In **1**, the two Fe(III)–O bonds have the same length within experimental error and the Fe1–O–Fe2 and Fe2–O–Fe3 angles differ by only 12.3° (Table II). To a first-order approximation, therefore, it is justified to assume the two Fe(II)–Fe(III) coupling constants J_{13} and J_{23} are equal. With $\mathbf{S}_1 = \mathbf{S}_2$, $g_1 = g_2$, and $J_{13} = J_{23} = J$, the Hamiltonian appropriate for the problem therefore reduces to eq 2, where $\mathbf{S}_{12} = \mathbf{S}_1 + \mathbf{S}_2$ and $\mathbf{S} = \mathbf{S}_{12} + \mathbf{S}_3$, J_{12} is the

$$\mathcal{H} = -2J_{12}\mathbf{S}_1\cdot\mathbf{S}_2 - 2J\mathbf{S}_{12}\cdot\mathbf{S}_3 + \mu_B[g_1\mathbf{S} + (g_3 - g_1)\mathbf{S}_3]\cdot\mathbf{H} \quad (2)$$

Fe(III)–Fe(III) exchange parameter, J is the Fe(II)–Fe(III) exchange parameter, g_1 the g factor for the two Fe(III) ions, and g_3 is that of the Fe(II) ion. General solutions for this problem have been given in the literature,[36,38] from which we obtained an expression for the theoretical susceptibility. Energy levels for the present system ($S_1 = S_2 = {}^5/_2$; $S_3 = 2$), obtained by using the first-order perturbation terms but neglecting higher order contributions, were inserted into the van Vleck equation.[35] Least-squares fits were carried out by using the program Model2.[43] Data points were weighted by σ^{-2}, where σ is the experimental error in the measured susceptibility obtained from duplicate measurements on the SQUID susceptometer.

A fit of the molar susceptibility of **1** to the appropriate expression gave $J = -16.5$ (4) cm^{-1}, $J_{12} = -41.8$ (10) cm^{-1}, and $g_3 = 2.22$ (1), where g_1 and g_2 were set equal to 2.0 and not varied. The theoretical curves are in excellent agreement with the experimental ones (Figure 4), justifying the use of only two J values to fit the data. The J_{12}:J ratio, which alone determines the ground state and sequence of exited states, is ~2.6.

The values of J and J_{12} are within the range reported previously for other $[Fe^{II}Fe^{III}_2O(O_2CR)_6L_3]$ mixed-valence compounds,[3] where the Fe(III)–Fe(III) exchange parameter J_{12} was always found to be about 2–3 times larger than the Fe(II)–Fe(III) exchange parameter J. A similar correlation seems to apply to oxo-bridged diiron cores.[7c,44] The larger number for J_{12} is consistent with the shorter Fe(III)–O compared to the Fe(II)–O bond lengths, in accord with the empirical relationship between the exchange parameter and the average Fe(III)–O bridge bond length derived previously.[42] From this expression, given in eq 3, we compute J_{12} to be −48.9 cm^{-1}, in reasonable agreement with the measured value of −41.8 cm^{-1}.

$$-J = 8.763 \times 10^{11} \exp(-12.663 \times \text{Fe–O}) \quad (3)$$

Inserting the J values into expressions for the energy reveals the ground state to have $S_T = 1$ ($S_{12} = 1$), as observed for most other $[Fe^{II}Fe^{III}_2O(O_2CR)_6L_3]$ compounds[36] and in agreement with the assignment made from the χ_M versus T plot. Only 15 cm^{-1} above the ground level lies the first excited state, which has S_T

(33) (a) Long, G. J.; Whitney, D. L.; Kennedy, J. E. *Inorg. Chem.* **1971**, *10*, 1406. (b) Ouseph, P. J.; Thomas, P. M.; Deszi, I. *J. Phys. Chem. Solids* **1974**, *35*, 604. (c) König, E.; Ritter, G.; Kulshreshtha, S. K.; Nelson, S. M. *Inorg. Chem.* **1982**, *21*, 3022.
(34) Robin, M. B.; Day, P. *Adv. Inorg. Chem. Radiochem.* **1967**, *10*, 247.
(35) Carlin, R. L. *Magnetochemistry*; Springer-Verlag: Berlin, 1986; p 6 ff.
(36) Ivleve, I. N.; Echmaev, S. B.; Stukan, R. A.; Turta, K. I.; Bobkova, S. A.; Veksel'man, M. E. *Russ. J. Inorg. Chem. (Engl. Transl.)* **1982**, *27*, 1479.
(37) Sinn, E. *Coord. Chem. Rev.* **1970**, *5*, 313.
(38) Tsukerblat, B. S.; Belinskl, M. I.; Ablov, A. V. *Akad. Nauk. SSSR, Dokl. Phys. Chem.* **1971**, *198*, 426.
(39) Blake, A. B.; Yavari, A.; Hatfield, W. E.; Sethuleksmi, C. N. *J. Chem. Soc., Dalton Trans.* **1985**, 2509.
(40) (a) Hay, J. P.; Thibeault, J. C.; Hoffmann, R. J. *J. Am. Chem. Soc.* **1975**, *97*, 4884. (b) Kahn, O.; Briat, B. *J. Chem. Soc., Faraday Trans. 2* 1976, 72. (c) Turowski, P. N.; Armstrong, W. H.; Roth, M. E.; Lippard, S. J. *J. Am. Chem. Soc.* **1990**, *112*, 681.
(41) Adler, J.; Ensling, J.; Gütlich, P.; Bomonaar, E. L.; Guillin, J.; Trautwein, A. X. *Hyperfine Interact.* **1988**, *42*, 869.
(42) (a) Gorun, S. M.; Lippard, S. J. *Recl. Trav. Chim. Pays-Bas* **1987**, *106*, 417. (b) Gorun, S. M.; Lippard, S. J. *Inorg. Chem.* **1991**, *30*, 1625.
(43) Vef. A. *Model2- Fit and Evaluation Program*; Institut für Anorganische Chemie und Analytische Chemie, Johannes-Gutenberg-Universität Mainz, 1989.
(44) DeWitt, J. G.; Bentsen, J. G.; Rosenzweig, A. C.; Hedman, B.; Green, J.; Pilkington, S.; Papaefthymiou, G. C.; Dalton, H.; Hodgson, K. O.; Lippard, S. J. Submitted for publication.

= 2 (2,0). This result explains the pronounced increase of the effective moment of **1** between 2 and 20 K, rising from 3.21 μ_B to 4.18 μ_B. The next two excited states ((2,1) and (0,2)) are $\sim$50 cm^{-1} above the (2,0) state.

Summary and Conclusions

The complex $[Fe_3O(O_2CCH_3)_6(TACN)]\cdot 2CHCl_3$ is the first example of an oxo-centered mixed-valence compound with ligands coordinating differently from those in the well-known $[Fe_3O(O_2CCH_3)_6L_3]$ class. The three monodentate ligands L are substituted by one tridentate L_3 molecule, shifting two of the bridging acetate ligands from bidentate bridging to bidentate terminal coordination mode. The stability of the $\{Fe_3O\}^{6+}$ core is underscored by the formation of **1** in an oxidative self-assembly reaction. Mössbauer spectroscopy as well as the X-ray crystal structure analysis show that **1** is a localized mixed-valence compound. Despite the fact that **1** has two geometrically distinct sites for the Fe(III) ions, the electronic properties of the two ferric ions seem to be very similar. Their Mössbauer parameters are nearly identical in the temperature range between 4.2 and 300 K, such that two quadrupole doublets are not resolved. The molar susceptibility of the antiferromagnetically coupled compound was successfully fit by using a model with only two different spin exchange coupling constants J. Compound **1** is also of interest as a rare example of an iron complex having terminal chelating carboxylate ligands and, as such, affords a useful structural benchmark for the dinuclear iron center in the B2 subunit of ribonucleotide reductase.

Acknowledgment. This work was supported by grants from the National Institute of General Medical Sciences and the National Science Foundation. P.P. thanks the Deutscher Akademischer Austauschdienst (DAAD) for a NATO Science Fellowship. G.C.P. acknowledges support by the Office of Naval Research, Program Cluster Sciences and Dynamics. The Francis Bitter National Magnet Laboratory was supported by the National Science Foundation.

Registry No. **1**·$2CHCl_3$, 133578-86-6.

Supplementary Material Available: Tables of positional parameters and B(eq) for all atoms, anisotropic thermal parameters for all non-hydrogen atoms, interatomic distances and angles, and experimental molar susceptibilities as a function of temperature for **1** (11 pages); observed and calculated structure factors for **1** (43 pages). Ordering information is given on any current masthead page.